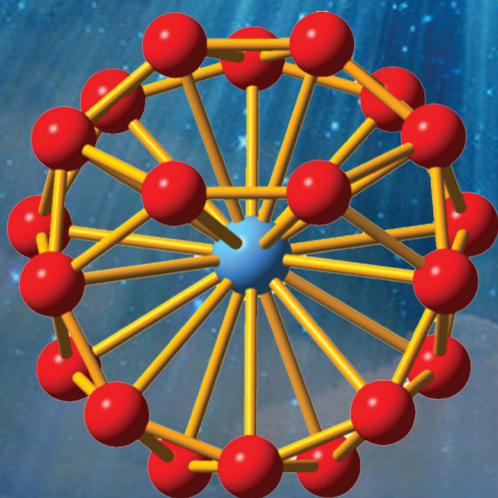


ChemComm

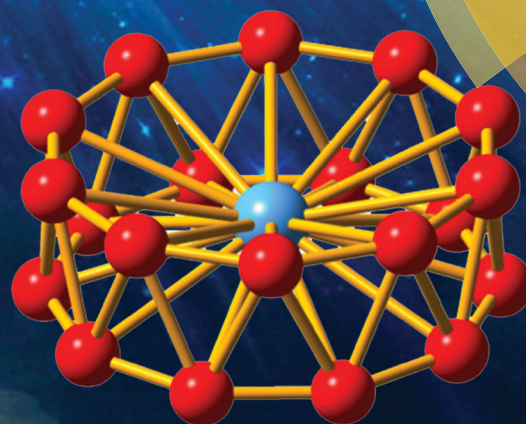
Chemical Communications

rsc.li/chemcomm

$[B_2-Ta@B_{18}]^-$



$[Ta@B_{20}]^-$



ISSN 1359-7345



ROYAL SOCIETY
OF CHEMISTRY

COMMUNICATION

Si-Dian Li, Jun Li, Lai-Sheng Wang *et al.*

Observation of a metal-centered B_2 - $Ta@B_{18}^-$ tubular molecular rotor and a perfect $Ta@B_{20}^-$ boron drum with the record coordination number of twenty



Cite this: *Chem. Commun.*, 2017, 53, 1587

Received 2nd December 2016,
Accepted 20th December 2016

DOI: 10.1039/c6cc09570d

www.rsc.org/chemcomm

Observation of a metal-centered B_2 -Ta@ B_{18}^- tubular molecular rotor and a perfect Ta@ B_{20}^- boron drum with the record coordination number of twenty†

Wan-Lu Li,^{‡a} Tian Jian,^{‡b} Xin Chen,^a Hai-Ru Li,^c Teng-Teng Chen,^b Xue-Mei Luo,^c Si-Dian Li,^{*c} Jun Li^{*a} and Lai-Sheng Wang^{*b}

A tubular molecular rotor B_2 -Ta@ B_{18}^- (1) and boron drum Ta@ B_{20}^- (2) with the highest coordination number of twenty in chemistry are observed via a joint photoelectron spectroscopy and first-principles theory investigation.

Boron has a vast variety of applications in structural chemistry and materials science owing to its electron deficiency.^{1,2} Over the past decade, the structures and chemical bonding of size-selected anionic boron clusters (B_n^-) have been systematically investigated through photoelectron spectroscopy (PES) in combination with theoretical calculations, revealing a rich structural landscape from planar sheets to fullerene-like cages (borospherenes).^{3–7} Boron cluster anions with up to 36 atoms have been proven to possess 2D global minimum structures,^{8–15} even though low-lying cage-like structures were also found for B_{28}^- and B_{29}^- .^{11,15} For cationic boron clusters (B_n^+), ion mobility in conjunction with density functional theory (DFT) calculations showed that double-ring tubular structures appeared at B_{16}^+ .¹⁶ In particular, the discovery of the planar $B_{36}^{0/-}$ and B_{35}^- clusters with hexagonal holes suggests the experimental feasibility of borophenes.^{13,14,17–20} The recent syntheses of borophenes on inert substrates^{21–23} pave the way for their applications in catalysis, 2D magnetism, and even possibly 2D superconductivity.^{24–26} Furthermore, the discovery of the cage-like $B_{40}^{-/0}$ and B_{39}^- borospherenes has enriched the diversity of boron nanostructures in analogy to the fullerenes.^{6,7}

Inspired by the findings of the planar wheel structures of the aromatic B_8^- and B_9^- clusters,²⁷ a series of transition-metal-doped boron wheels ($M@B_n^-$, $n = 8–10$) were produced and

characterized both experimentally and theoretically.²⁸ It has been concluded that the NbB_{10}^- and TaB_{10}^- clusters have the highest possible coordination number in planar species.^{29,30} Two larger metal-doped boron clusters, CoB_{12}^- and RhB_{12}^- , were found to adopt half-sandwich type structures.³¹ Large metal-doped boron clusters have also been investigated computationally.^{32–34}

Recently, the CoB_{16}^- and MnB_{16}^- clusters have been found to have remarkable drum-like structures.^{35,36} However, the CoB_{18}^- cluster is found to be planar with Co being an integral part of the boron triangular lattice,³⁷ suggesting the possibility of metallo-borophenes.^{38,39} When Co is substituted with the larger Rh atom, a perfect D_{9d} RhB_{18}^- drum was observed.⁴⁰ An interesting question arises: can even larger boron drums with a central metal atom be formed?

Given the fact that Ta dopant has given the largest molecular wheel previously,^{28–30} we perform a joint PES and *ab initio* investigation on TaB_{20}^- in this work. Theoretical results based on both DFT and wave function theory indicate that a metal-centred tubular molecular rotor (C_s , isomer 1) with a B_2 unit rotating over the B_{18} drum (B_2 -Ta@ B_{18}^-) is the global minimum and is the carrier of the main PES features observed experimentally, while a perfect metal-centred drum-like Ta@ B_{20}^- (D_{10d} , isomer 2) lies only 0.81 kcal mol⁻¹ higher in energy and coexists in the experiment as a minor isomer.

The TaB_{20}^- cluster was produced by a laser vaporization supersonic cluster source and mass-selected using time-of-flight mass spectrometry before being photodetached at 266 nm and 193 nm (see Photoelectron Spectroscopy Experiment in the ESI†).³ The photoelectron spectra are shown in Fig. 1, where the 193 nm spectrum displays five intense and broad features (X, A–D) and a discernible weak band labeled as X'. The vertical detachment energies (VDEs) of these bands are summarized in Table S1 (ESI†), where they are compared with theoretical VDEs. Peak X with a VDE of 3.30 eV represents the detachment transition from the ground state of the anion to that of the neutral. The adiabatic detachment energy (ADE) of peak X was estimated to be 2.95 ± 0.05 eV from its onset in the 266 nm spectrum (Fig. 1a). The peak X' with a VDE of 3.63 eV was right

^a Department of Chemistry and Key Laboratory of Organic Optoelectronics & Molecular Engineering of Ministry of Education, Tsinghua University, Beijing 100084, China. E-mail: junli@tsinghua.edu.cn

^b Department of Chemistry, Brown University, Providence, RI 02912, USA. E-mail: Lai-Sheng_Wang@brown.edu

^c Institute of Molecular Science, Shanxi University, Taiyuan 030006, China. E-mail: lisidian@sxu.edu.cn

† Electronic supplementary information (ESI) available. See DOI: 10.1039/c6cc09570d

‡ These authors contributed equally to this work.

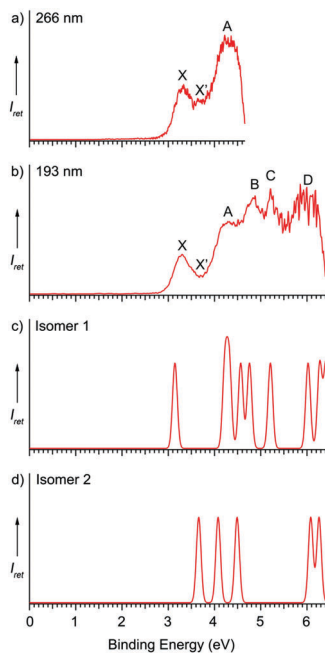


Fig. 1 Photoelectron spectra of TaB_{20}^- at 266 nm (4.661 eV) (a) and 193 nm (6.424 eV) (b) and comparison with simulated spectra of isomers **1** (c) and **2** (d) at the SAOP/TZP level.

in between bands X and A and it was slightly better resolved in the 266 nm spectrum. Its weak intensity suggested that it was likely originated from a weakly populated TaB_{20}^- isomer in the cluster beam. The broad band A at 4.29 eV is separated from band X by an energy gap of ~ 1 eV. Bands B and C at 4.86 and 5.22 eV, respectively, were slightly sharper. A very broad band D at 6 eV was observed. Overall, the PE spectra of TaB_{20}^- exhibited well-resolved bands and suggested the co-existence of a minor isomer.

To locate the global minimum of the TaB_{20}^- , we performed extensive global searches followed by first-principles calculations (see Computational Details in ESI†). Isomers within ~ 35 kcal mol $^{-1}$ above the global minima are presented in Fig. S1 (ESI†) accompanied with some representative structures with higher relative energies. Encouragingly, all levels of theory predicted that isomer **1** (C_s , $^1A_1'$) is the global minimum of the TaB_{20}^- cluster, revealing a Ta-centered eighteen-membered drum with a B_2 unit on the top, $[(B_2\text{-Ta}@B_{18})^-]$ (Fig. 2). The second lowest-lying isomer **2** is a perfect twenty-membered boron drum (D_{10d} , 1A_1), which lies only 0.81 kcal mol $^{-1}$ higher above the global minimum at the CCSD(T) level.^{41,42} With such a small relative energy, isomers **1** and **2** can be viewed as almost generate and they are expected to coexist in the experiment. The next two isomers **3** and **4** are well separated from isomers **1** and **2** energetically, lying 16.95 and 11.30 kcal mol $^{-1}$ higher than isomer **1**, respectively (Fig. S1 and S2, ESI†). Thus, the two lowest energy isomers **1** and **2** are considerably more stable than any other structures and should be the only isomers accessible experimentally.

The configurational energy spectrum of TaB_{20}^- within 70 kcal mol $^{-1}$ from the PBE/TZP method^{43,44} is presented in Fig. S2 (ESI†). The quasi-planar **70** (C_1 , 1A_1) with a nonacoordinate

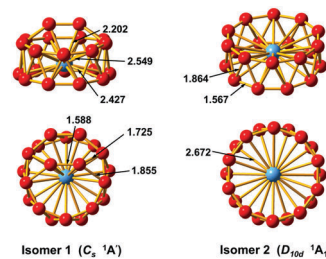


Fig. 2 Front and top views of isomers **1** and **2** of TaB_{20}^- at PBE0/TZP.

Ta and **104** (C_1 , 1A_1) with an octacoordinate Ta appear to be totally uncompetitive in energy, lying 56.43 and 69.09 kcal mol $^{-1}$ higher than **1**, respectively. The two eighteen-membered drum structures **5** (C_s , $^1A_1'$) and **32** (C_1 , 1A_1), in which the two B atoms situate outside of the drum framework possess the relative energies of 15.13 and 33.70 kcal mol $^{-1}$, respectively. A sixteen-membered drum (**87**) with a B_4 square at the top was also found to lie 64.36 kcal mol $^{-1}$ higher than **1**.

To facilitate comparisons with the experimental results, we calculated the VDEs of isomers **1** and **2** using the relativistic $\Delta\text{SCF-TDDFT}$ method⁴⁵ with the SAOP density functional,⁴⁶ which has proved to produce accurate excitation energies for metal-doped boron clusters.^{36,37,40} The first VDEs and ADEs calculated using the PBE/TZP, PBE0/TZP,⁴⁷ and CCSD(T) methods are given in Table S2 (ESI†) compared with the experimental data. Clearly, the CCSD(T) results are in better agreement with the experiment. The higher theoretical VDEs are compared with the experimental data in Table S1 (ESI†). The theoretical first ADE/VDE (3.05/3.14 eV) of isomer **1** agree well with the X feature with ADE/VDE of 2.95/3.30 eV, which represents electron detachment from the $54a'$ HOMO (Fig. S3, ESI†). The large energy gap (0.90 eV) between the HOMO and HOMO-1 ($53a'$) in isomer **1** is consistent with the large separation between the X and A bands (Fig. 1). The HOMO is mainly of B character, whereas the HOMO-1 is mainly derived from the head-to-head overlap between Ta $5d_{z^2}$ and the p_π orbital of the B_2 unit in the vertical direction. Bands A and B correspond to four detachment channels from isomer **1** (Fig. 1c and Table S1, ESI†). Band C corresponds to a single detachment channel from the $51a'$ orbital. At least three detachment channels contribute to the broad band D. The calculated VDEs and the simulated PES for isomer **1** of TaB_{20}^- are in good agreement with the main observed features (X, A-D).

The theoretical first VDE of isomer **2** was 3.66 eV, in excellent agreement with X' at 3.63 eV. The high symmetry **2** generates only four more detachment channels within the experimental energy range. These features were likely buried in the strong PES signals from the dominating isomer **1**. Hence, the combined theoretical results from isomers **1** and **2** are in excellent agreement with the experimental PES, providing considerable credence for the coexistence of the major isomer **1** and minor isomer **2**.

The optimized structures of the two lowest-lying isomers **1** and **2** are detailed in Fig. 2. Isomer **1** is composed of a Ta-centered eighteen-membered drum and two bridging B atoms atop the drum, forming a B_6 hexagon on the top involving the B_2 unit and four periphery B atoms on the $\text{Ta}@B_{18}$ drum motif. The Ta-B

distances are calculated to be 2.427–2.549 Å in the Ta@B₁₈ drum unit in isomer **1** and the bond lengths between the central Ta and the two equivalent B atoms in the B₂ unit are even shorter (2.202 Å). The Ta–B distance of the D_{10d} **2** is calculated to be 2.672 Å, which is longer than 2.31 Å based on the sum of the single-bond covalent radii of Ta and B recommended by Pyykkö.⁴⁸ These calculated Ta–B distances are close to the corresponding value of 2.47 Å in the previously reported monocyclic complex Ta@B₁₀[−].²⁹ Clearly, there exist effective coordination interactions between the Ta center and the surrounding twenty B atoms in both **1** and **2** (see Table S2 for detailed bond orders, ESI†). The central Ta atom in both isomers **1** and **2** is thus unprecedentedly coordinated by twenty B atoms. It is noticed that isomer **2** with the tube diameter of 5.26 Å is the largest embryo for boronanotubes reported to date.^{35,36,40,49} The slightly higher stability of isomer **1** implies that the twenty-membered double-layer drum **2** has likely reached the size limit in diameter for metallo-boronanotubes.

Using the spin-restricted open-shell ROCCSD(T) method, we computed the binding energies of Ta(5d³6s²) + B₂₀[−](²B₂/²A) → Ta@B₂₀[−](¹A₁/¹A) which turned out to be 274.4 kcal mol^{−1} and 252.1 kcal mol^{−1} for isomer **1** and **2**, respectively. Moreover, various calculated bond indices also give appreciable values to support the existence of effective coordination interactions between Ta and B. Both the total bond order of the Ta center and the average bond order of boron atoms in isomer **1** are higher than the corresponding values in isomer **2**, consistent with the slightly higher stability of **1** with respect to **2**. As shown in Table S2 (ESI†), the Ta–B interactions involving the B₂ unit in **1** possess much higher Wiberg bond orders⁵⁰ (0.53) than that involving the B₁₈ drum (0.26): the two equivalent Ta–B coordination bonds in the Ta–B₂ triangle combined together may be effectively viewed as a 3c–2e covalent bond, whereas the Ta–B₁₈ interactions belong to typical coordination bonds comparable with the Fe–C interaction (0.30) in ferrocene (C₅H₅)₂Fe.

The bonding pattern of isomer **1** is shown using the Kohn–Sham orbitals in Fig. S3 (ESI†). The top B₂ unit is stabilized significantly by the interaction of the B₂ p_π with the Ta 5d_{z²} and 5d_{yz} hybridized orbitals (51a' and 53a'), whereas the B₁₈ drum is bonded with the central Ta *via* three delocalized orbitals involving the 2p_r orbitals of the B₁₈ skeleton and the Ta 5d_{xy}/d_{xz}/d_{x²−y²} orbitals (31a'', 50a', and 32a''). The observation of isomer **1** raises an interesting question whether a bare D_{9d} Ta@B₁₈[−] drum is possible. It turned out to be an open-shell with two unpaired electrons in the degenerate 6e_g HOMOs (Fig. S4 (ESI†)). Addition of two extra electrons makes a stable closed-shell TaB₁₈^{3−} species. The two electrons can be transferred from the B₂ unit in B₂-Ta@B₁₈[−] (**1**), making it the global minimum of the monoanion.

The chemical bonding of the perfect D_{10d} Ta@B₂₀[−] drum was analyzed using the AdNDP method,⁵¹ as shown in Fig. S5 (ESI†). The first row shows 20 B–B 2c–2e σ bonds within the two staggered B₁₀ rings. The second row exhibits three 20c–2e σ + σ bonding orbitals (b and c), between the two B₁₀ moieties. The 20c–2e bond in the third row (e) exhibits delocalized σ bonding character within each B₁₀ ring, but antibonding character between the two B₁₀ rings. The two 21c–2e bonds in

the second row (d) involve both inter-ring σ + σ interactions, as well as σ bonding interactions between the Ta 5d_{xy} and 5d_{x²−y²} orbitals and the B₁₀ rings. The two 21c–2e bonds in the third row (f) involve primarily bonding between the Ta 5d_{xz} and 5d_{yz} orbitals and the surrounding boron. The fourth row describes five delocalized π–π bonds (g, h, and i) between the two B₁₀ rings. The second to fourth row each describes an aromatic system, resulting in a fairly stable D_{10d} Ta@B₂₀[−] drum.

The B₂ unit atop the Ta@B₁₈[−] drum in the global minimum of TaB₂₀[−] is quite unusual and surprising. The B–B bond within the B₂ dimer is strong with a bond length of 1.588 Å (Fig. 2). But the bonding between the B₂ dimer and the drum periphery is relatively weak with two inequivalent B–B distances (1.725 and 1.855 Å). Given the fact that there exist nine available B sites on the B₁₈ drum periphery, an interesting question is whether the B₂ unit can rotate relative to the Ta@B₁₈ drum motif. To understand the energy barriers along the rotational process, we searched for the possible transition state (TS) between two adjacent structures of isomer **1**.

A first-order C_s stationary structure (Fig. S6, ESI†) was located as the TS with one imaginary frequency of 93i cm^{−1} at PBE0/VTZ.⁵² The C_s TS features a B₅ pentagon on the drum top involving the B₂ unit and three periphery B atoms on the Ta@B₁₈ drum motif. The energy barrier was calculated to be only 1.13 kcal mol^{−1} at the CCSD(T)/VTZ⁵³. Extensive molecular dynamics simulations indicate that the B₂ unit rotates almost freely around the molecular axis of the Ta@B₁₈ drum at 900 K (Fig. S7 and Video S1 (ESI†)). There exist nine equivalent positions to form the global minima (GM_{*i*}, *i* = 1–9) on the potential energy surface during the rotation in a full circle, with a rotation angle of 40° for each step. Correspondingly, nine equivalent transition structures TS_{*i*−*j*} (*i*, *j* = 1–9) are formed between the nine global minima. Thus, isomer **1** of TaB₂₀[−] can be described as a tubular molecular rotor. When the rotor forms a hexagonal hole on the drum top, the system reaches its global minimum. Conversely, the system arrives at a transition state when the hole becomes pentagonal. Internal rotations in planar boron clusters have been found previously in B₁₉[−], B₁₃⁺, and B₁₈^{2−}.^{54–57} Rotations of carbon fragments inside a series of planar C–B clusters (C₂B₈, C₃B₉³⁺, and C₅B₁₁⁺) have also been considered computationally.⁵⁸ However, these C–B clusters were hypothetical because carbon has been shown to prefer peripheral sites in carbon-doped boron clusters.^{59–61} The tubular B₂-Ta@B₁₈[−] (**1**) presents a new type of internal rotation fundamentally different from the basket-like [B₂-C₂B₈H₁₂]^{2−} which is a transition state in the isomerization of [C₂B₁₀H₁₂]^{2−}.⁶²

In summary, we have reported a joint experimental and theoretical investigation of a relatively large metal-doped boron cluster, TaB₂₀[−], which is found to possess a unique tubular molecular rotor C_s B₂-Ta@B₁₈[−] (**1**) as the global minimum. A perfect D_{10d} Ta@B₂₀[−] nano-drum (**2**) is observed as a minor isomer. Both isomers possess the record coordination number of twenty unknown in any other chemical compounds. B₂-Ta@B₁₈[−] (**1**) represents the structural transition from tubular to cage-like in metal-doped boron clusters, while Ta@B₂₀[−] (**2**) has likely reached the size limit in diameter for metallo-boronanotubes.

The experimental PES work done at Brown University was supported by the US National Science Foundation (CHE-1632813). The theoretical work done at Tsinghua University and Shanxi University was supported by NKBRSF (2013CB834603) and NSFC (21433005, 91426302, 21521091, 21590792, and 21373130).

Notes and references

- W. N. Lipscomb, *Science*, 1977, **196**, 1047–1055.
- B. Albert and H. Hillebrecht, *Angew. Chem., Int. Ed.*, 2009, **48**, 8640–8668.
- L. S. Wang, *Int. Rev. Phys. Chem.*, 2016, **35**, 69–142.
- A. N. Alexandrova, A. I. Boldyrev, H. J. Zhai and L. S. Wang, *Coord. Chem. Rev.*, 2006, **250**, 2811–2866.
- A. P. Sergeeva, I. A. Popov, Z. A. Piazza, W. L. Li, C. Romanescu, L. S. Wang and A. I. Boldyrev, *Acc. Chem. Res.*, 2014, **47**, 1349–1358.
- H. J. Zhai, Y. F. Zhao, W. L. Li, Q. Chen, H. Bai, H. S. Hu, Z. A. Piazza, W. J. Tian, H. G. Lu, Y. B. Wu, Y. W. Mu, G. F. Wei, Z. P. Liu, J. Li, S. D. Li and L. S. Wang, *Nat. Chem.*, 2014, **6**, 727–731.
- Q. Chen, W. L. Li, Y. F. Zhao, S. Y. Zhang, H. S. Hu, H. Bai, H. R. Li, W. J. Tian, H. G. Lu, H. J. Zhai, S. D. Li, J. Li and L. S. Wang, *ACS Nano*, 2015, **9**, 754–760.
- A. P. Sergeeva, D. Y. Zubarev, H. J. Zhai, A. I. Boldyrev and L. S. Wang, *J. Am. Chem. Soc.*, 2008, **130**, 7244–7246.
- W. Huang, A. P. Sergeeva, H. J. Zhai, B. B. Averkiev, L. S. Wang and A. I. Boldyrev, *Nat. Chem.*, 2010, **2**, 202–206.
- W. L. Li, R. Pal, Z. A. Piazza, X. C. Zeng and L. S. Wang, *J. Chem. Phys.*, 2015, **142**, 204305.
- H. R. Li, T. Jian, W. L. Li, C. Q. Miao, Y. J. Wang, Q. Chen, X. M. Luo, K. Wang, H. J. Zhai, S. D. Li and L. S. Wang, *Phys. Chem. Chem. Phys.*, 2016, **18**, 29147–29155.
- W. L. Li, Y. F. Zhao, H. S. Hu, J. Li and L. S. Wang, *Angew. Chem., Int. Ed.*, 2014, **53**, 5540–5545.
- W. L. Li, Q. Chen, W. J. Tian, H. Bai, Y. F. Zhao, H. S. Hu, J. Li, H. J. Zhai, S. D. Li and L. S. Wang, *J. Am. Chem. Soc.*, 2014, **136**, 12257–12260.
- Z. A. Piazza, H. S. Hu, W. L. Li, Y. F. Zhao, J. Li and L. S. Wang, *Nat. Commun.*, 2014, **5**, 3113.
- Y. J. Wang, Y. F. Zhao, W. L. Li, T. Jian, Q. Chen, X. R. You, T. Ou, X. Y. Zhao, H. J. Zhai, S. D. Li, J. Li and L. S. Wang, *J. Chem. Phys.*, 2016, **144**, 064307.
- E. Oger, N. R. M. Crawford, R. Kelting, P. Weis, M. M. Kappes and R. Ahlrichs, *Angew. Chem., Int. Ed.*, 2007, **46**, 8503–8506.
- H. Tang and S. Ismail-Beigi, *Phys. Rev. Lett.*, 2007, **99**, 115501.
- X. Yang, Y. Ding and J. Ni, *Phys. Rev. B: Condens. Matter Mater. Phys.*, 2008, **77**, 041402.
- E. S. Penev, S. Bhowmick, A. Sadrzadeh and B. I. Yakobson, *Nano Lett.*, 2012, **12**, 2441–2445.
- X. J. Wu, J. Dai, Y. Zhao, Z. W. Zhuo, J. L. Yang and X. C. Zeng, *ACS Nano*, 2012, **6**, 7443–7453.
- A. J. Mannix, X. F. Zhou, B. Kiraly, J. D. Wood, D. Alducin, B. D. Myers, X. L. Liu, B. L. Fisher, U. Santiago, J. R. Guest, M. J. Yacaman, A. Ponce, A. R. Oganov, M. C. Hersam and N. P. Guisinger, *Science*, 2015, **350**, 1513–1516.
- B. J. Feng, J. Zhang, Q. Zhong, W. B. Li, S. Li, H. Li, P. Cheng, S. Meng, L. Chen and K. H. Wu, *Nat. Chem.*, 2016, **8**, 563–568.
- S. Xu, Y. Zhao, J. Liao, X. Yang and H. Xu, *Nano Res.*, 2016, **9**, 2616–2622.
- E. S. Penev, A. Kutana and B. I. Yakobson, *Nano Lett.*, 2016, **16**, 2522–2526.
- M. Gao, Q. Z. Li, X. W. Yan and J. Wang, arXiv:1602.02930v1.
- R. C. Xiao, D. F. Shao, W. J. Lu, H. Y. Lv, J. Y. Li and Y. P. Sun, *Appl. Phys. Lett.*, 2016, **109**, 122604.
- H. J. Zhai, A. N. Alexandrova, K. A. Birch, A. I. Boldyrev and L. S. Wang, *Angew. Chem., Int. Ed.*, 2003, **42**, 6004–6008.
- C. Romanescu, T. R. Galeev, W. L. Li, A. I. Boldyrev and L. S. Wang, *Acc. Chem. Res.*, 2013, **46**, 350–358.
- T. R. Galeev, C. Romanescu, W. L. Li, L. S. Wang and A. I. Boldyrev, *Angew. Chem., Int. Ed.*, 2012, **51**, 2101–2105.
- T. Heine and G. Merino, *Angew. Chem., Int. Ed.*, 2012, **51**, 4275–4276.
- I. A. Popov, W. L. Li, Z. A. Piazza, A. I. Boldyrev and L. S. Wang, *J. Phys. Chem. A*, 2014, **118**, 8098–8105.
- C. Xu, L. J. Cheng and J. L. Yang, *J. Chem. Phys.*, 2014, **141**, 124301.
- N. M. Tam, H. T. Pham, L. V. Duong, M. P. Pham-Ho and M. T. Nguyen, *Phys. Chem. Chem. Phys.*, 2015, **17**, 3000–3003.
- J. Lv, Y. C. Wang, L. J. Zhang, H. Q. Lin, J. J. Zhao and Y. M. Ma, *Nanoscale*, 2015, **7**, 10482–10489.
- I. A. Popov, T. Jian, G. V. Lopez, A. I. Boldyrev and L. S. Wang, *Nat. Commun.*, 2015, **6**, 8654.
- T. Jian, W. L. Li, I. A. Popov, G. V. Lopez, X. Chen, A. I. Boldyrev, J. Li and L. S. Wang, *J. Chem. Phys.*, 2016, **144**, 154310.
- W. L. Li, T. Jian, X. Chen, T. T. Chen, G. V. Lopez, J. Li and L. S. Wang, *Angew. Chem., Int. Ed.*, 2016, **55**, 7358–7363.
- H. Zhang, Y. Li, J. Hou, K. Tu and Z. Chen, *J. Am. Chem. Soc.*, 2016, **138**, 5644–5651.
- H. Zhang, Y. Li, J. Hou, A. Du and Z. Chen, *Nano Lett.*, 2016, **16**, 6124–6129.
- T. Jian, W. L. Li, X. Chen, T. T. Chen, G. V. Lopez, J. Li and L. S. Wang, *Chem. Sci.*, 2016, **7**, 7020–7027.
- G. D. Purvis III and R. J. Bartlett, *J. Chem. Phys.*, 1982, **76**, 1910–1918.
- G. E. Scuseria, C. L. Janssen and H. F. Schaefer III, *J. Chem. Phys.*, 1988, **89**, 7382–7387.
- J. P. Perdew, K. Burke and M. Ernzerhof, *Phys. Rev. Lett.*, 1996, **77**, 3865–3868.
- E. van Lenthe and E. J. Baerends, *J. Comput. Chem.*, 2003, **24**, 1142–1156.
- S. J. A. van Gisbergen, J. G. Snijders and E. J. Baerends, *Comput. Phys. Commun.*, 1999, **118**, 119–138.
- P. R. T. Schipper, O. V. Gritsenko, S. J. A. van Gisbergen and E. J. Baerends, *J. Chem. Phys.*, 2000, **112**, 1344–1352.
- C. Adamo and V. Barone, *J. Chem. Phys.*, 1999, **110**, 6158–6170.
- P. Pyykkö, *J. Phys. Chem. A*, 2015, **119**, 2326–2337.
- B. Kiran, S. Bulusu, H. J. Zhai, S. Yoo, X. C. Zeng and L. S. Wang, *Proc. Natl. Acad. Sci. U. S. A.*, 2005, **102**, 961–964.
- K. B. Wiberg, *Tetrahedron*, 1968, **24**, 1083–1096.
- D. Y. Zubarev and A. I. Boldyrev, *Phys. Chem. Chem. Phys.*, 2008, **10**, 5207–5217.
- T. H. Dunning, *J. Chem. Phys.*, 1989, **90**, 1007–1023.
- D. Figgen, K. A. Peterson, M. Dolg and H. Stoll, *J. Chem. Phys.*, 2009, **130**, 164108.
- J. O. C. Jimenez-Halla, R. Islas, T. Heine and G. Merino, *Angew. Chem., Int. Ed.*, 2010, **49**, 5668–5671.
- G. Martinez-Guajardo, A. P. Sergeeva, A. I. Boldyrev, T. Heine, J. M. Ugalde and G. Merino, *Chem. Commun.*, 2011, **47**, 6242–6244.
- J. Zhang, A. P. Sergeeva, M. Sparta and A. N. Alexandrova, *Angew. Chem., Int. Ed.*, 2012, **51**, 8512–8515.
- D. Moreno, S. Pan, L. L. Zeonjuk, R. Islas, E. Osorio, G. Martinez-Guajardo, P. K. Chattaraj, T. Heine and G. Merino, *Chem. Commun.*, 2014, **50**, 8140–8143.
- S. Erhardt, G. Frenking, Z. Chen and P. V. R. Schleyer, *Angew. Chem., Int. Ed.*, 2005, **44**, 1078–1082.
- L. M. Wang, W. Huang, B. B. Averkiev, A. I. Boldyrev and L. S. Wang, *Angew. Chem., Int. Ed.*, 2007, **46**, 4550–4553.
- B. B. Averkiev, D. Y. Zubarev, L. M. Wang, W. Huang, L. S. Wang and A. I. Boldyrev, *J. Am. Chem. Soc.*, 2008, **130**, 9248–9250.
- B. B. Averkiev, L. M. Wang, W. Huang, L. S. Wang and A. I. Boldyrev, *Phys. Chem. Chem. Phys.*, 2009, **11**, 9840–9849.
- D. Mckay, S. A. Macgregor and A. J. Welch, *Chem. Sci.*, 2015, **6**, 3117–3128.